EXPERIMENTAL STUDIES OF SOME FEATURES OF BEAM-PLASMA DISCHARGE INITIAL STAGE

V.I. Butenko, B.I. Ivanov, V.P. Prishchepov
NSC KIPT, Kharkov, 61108, Ukraine (E-mail: ivanovbi@kipt.kharkov.ua)

In case of gas pressure increasing, the plasma density rapidly increases at p=(1-2)*10^{-4} Torr, due to the beam-plasma discharge start (BPD). For fixed pressure above 2*10^{-4} Torr, the BPD start depends from the interaction length L and beam current I, with relation $I \propto L^{-1}$. Measurements of the electron velocity distribution were performed using an UHF method and a multi-electrode probe. The start conditions are agreed with theoretical estimations.
PACS: 52.40.Mj

1. EXPERIMENTS

Beam-plasma studies were described in many papers and reviews (e. g., see [1]). Our paper is devoted to a particular problem, namely, to the start conditions of beam-plasma discharges (BPG). This problem was investigated in [-]. In [2,3] BPD was studied for the cyclotron branch. In this case the BPD start (for hydrogen gas) take place at the pressure of (1-2)*10^{-4} Torr [2]; in [3] the BPD start (for nitrogen and argon) take place at the pressure ~1*10^{-4} Torr. In [4-6], where BPD was studied for the plasma branch, the discharge also starts at the pressure of (1-2)*10^{-4} Torr. Our studies were performed on three different installations. It is interesting to note that all these experiments demonstrate the BPD start at the same critical pressure, p_{cr}=(1-2)*10^{-4} Torr. This phenomenon requires further investigations and explanations.

Parameters of our first installation (see Fig. 1): a pulsed axial electron beam of 0-12 keV, 0-3 A, 10 mm diameter; pulse duration 25 mks, a longitudinal magnetic field of 0,1-1 kOe; an interaction length is 40 cm.

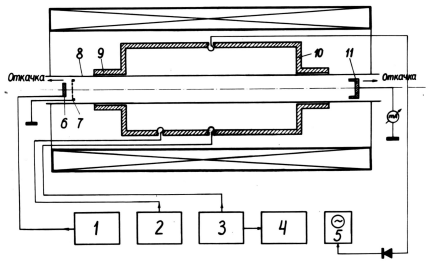

Fig. 1. 1-15 kV rectifier, 2-pulse forming line, 3-start device, 4-400 V rectifier...7-HF oscillator…12-cathode, 13-anode, 14-collector, 15-quartz tube, 16-HF cavity

In case of increasing gas pressure (air) up to 10^{-4} Torr, the BPG starts, and the electron density quickly rises from 2.7*10^{9} cm^{-3} to 1.1*10^{10} cm^{-3} (*Fig. 2*).

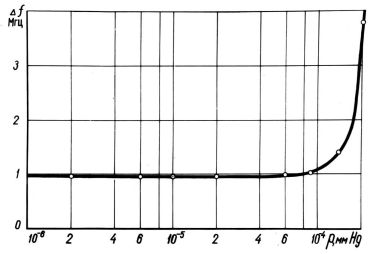

*Fig. 2. Frequency shift for a HF-cavity vs. pressure for 10 keV beam (Δf=1 MHz corresponds to n=2.7*10^{9} cm^{-3})*

The electron distribution function of BPD was measured at 2nd installation, see Fig. 3. The electron beam was created by a gun consisting of a LaB_6 cathode (11) and a mesh anode (12), with the following parameters:

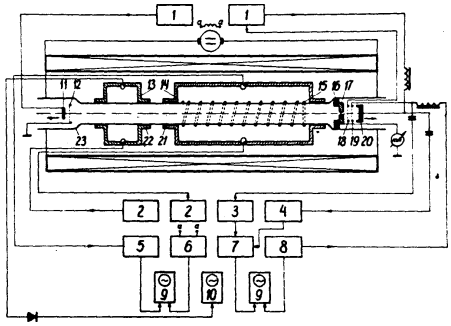

Fig. 3. Setup of 2nd installation

DC beam voltage U~10-1000 V, current I~1-100 mA, beam diameter 2a =10 mm, magnetic field H variable between 0 and 1 kOe , magnetic field inhomogenity 1 %. The beam was shot down the axis of a quartz tube 30 mm in diameter, which was evacuated down to pressures of the order of 10^{-6} Torr. A cavity operated in the E_{010} mode (13) was mounted coaxial with the tube and served to measure electron density, together with an axially overmode helical resonator (14) which was used for the measurement of the distribution of electrons over axial velocity. The parameters of the helical resonator are: I.D. of metallic screen 2b=102 mm, height h=300 mm,; helix I.D. 2c=33 mm, helix pitch 17 mm. The resonator was excited via a coupling loop from a generator (2) delivering 10 mW at the resonant frequency f=1750 MHz, v_{ph}/c=0.4, and k_3=0.8 cm^{-1}. The microwave power transmitted through the resonator was registered with a receiver (5) and oscilloscope (9). The magnetic field was varied linearly in time, by means of a sawtooth generator (6). The microwave power transmitted through the resonator was displayed on the scope screen vs. magnetic field.

We have simultaneously measured the distribution function by means of the multi-electrode probe. To measure the energy distribution by means of the retarding potential method we have to differentiate collector current with respect to analyzing grid voltage: $f(W_{||}) \propto dI_k / dU_e$. We have used a setup permitting to carry out such differentiation and to display the distribution function on the scope screen. Fig. 4 (oscillograms 2,4,6) shows these electron energy distribution function in the beam-plasma discharge (lower trace). The upper trace is the variation of voltage on the analyzing grid. On the left are the oscillograms (1, 3, 5) of microwave power transmitted through the resonator vs. magnetic field (lower trace). The upper

trace is the variation of magnetic field strength. The parameter is the residual gas pressure. As the pressure is increased the beam cyclotron absorption peak merges with the plasma peak, and a characteristic plateau is formed in the distribution function (see oscillograms 5,6).

Fig. 5 a,b is a comparison of electron distribution measurements in the initial stage of the beam-plasma discharge, by the microwave method and the retarding potential method. The oscillograms (1) are $[P(H)]^{1/2}$ curves used to calculate $f(v_{||})$ curves (2) and the oscillograms (3) are distribution functions $f(W_{||})$ obtained by the retarding potential method. In the initial stage of the discharge both methods give like results.

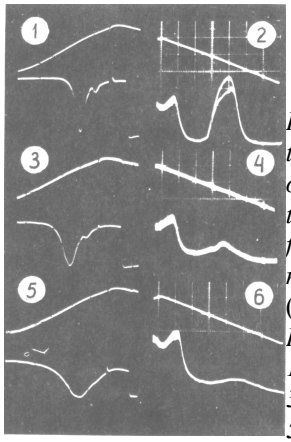

*Fig. 4. Dependence of transmitted microwave power on magnetic field strength, and the electron distribution function, measured with the retarding potential method (U = 300 V, I = 10 mA, H = 400 - 700 Oe; 1,2 - n = 2.8*10^8 cm^{-3}; 3,4 -n=4.6*10^8 cm^{-3}; 5,6-n=8.3*10^8 cm^{-3})*

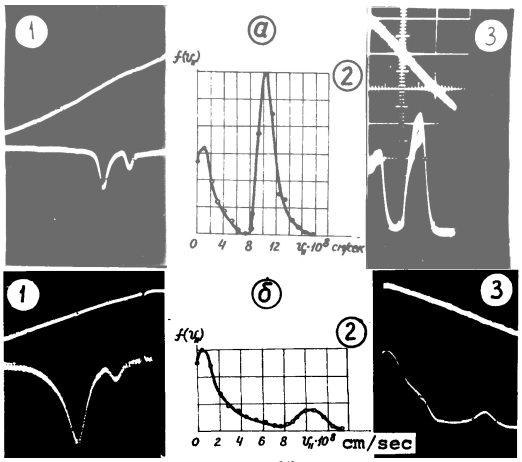

*Fig. 5. The function $[P(H)]^{1/2}$ (1) and the electron distribution function, measured with the microwave method (2) and the retarding potential method (3). (U=300 V, I=10 mA, H = 400-700 Oe, U_3= -(0-600) V. a) n =10^8 cm^{-3} ; b) n = 3.7*10^8 cm^{-3})*

The scheme of the 3rd experimental set is presented in Fig. 6. Electron beam was created by electron gun with LaB_6 cathode (1) of 3 cm diameter and anode grid (2).

The DC energy and current of the beam were changed in the interval 0-10 keV, 0-60 mA. Through the pipe (3) providing pressure jump, electron beam was injected into interaction chamber (4) of 150 cm length and 15 cm diameter. Inside of it there are placed: an open 8 mm resonator (5) for plasma density measurement, HF-probes (6),

a movable metallic screen beam collector (7). Interaction chamber was placed in solenoid creating magnetic field up to 1500 Oe. The HF-probes were two double-wound magnetic loops, oriented on azimuthal and longitudinal components of HF magnetic field. Movable copper screen of 13 cm diameter provides the length changing of the beam-plasma interaction region. Plasma was produced during interaction of electron beam with neutral gas.

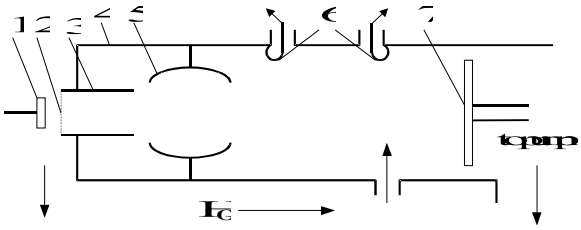

Fig. 6. 3rd experimental set (1, 2 - cathode and anode of electron gun, 3-pressure jump pipe, 4-interaction chamber, 5-resonator, 6-HF-probes, 7-movable beam collector

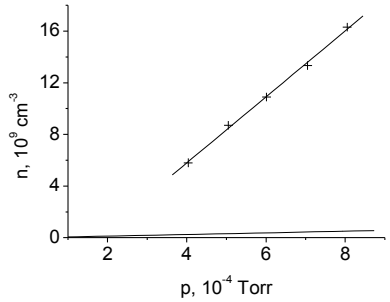

Fig. 7. Plasma density dependence vs. gas pressure (bottom - collision ionization, top – ionization by BPD)

In Fig. 7 the plasma density on dependence of gas pressure is presented. Here the BPD starts at p=2*10^{-4} Torr.

The start current I_{st} dependence on the interaction length L is shown in Fig. 8; as it is follows, $I_{st} \propto AL^{-1}$.

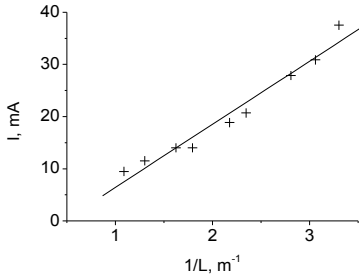

Fig. 8. Start current vs. interaction length in form of L^{-1}

The growth rates of excited oscillations were found near the plasma frequency: $\omega \leq \omega_p$ and the cyclotron frequency: $\omega \geq \omega_H$. In Fig. 9 series of spectra are presented for the beam current values. Magnetic field is 700 Oe, beam energy 2 keV, interaction length 122 cm, gas pressure 5·10^{-4} Torr. It is seen that spectrum has two maxima corresponding to frequency bands for case of $\omega_p < \omega_H$.

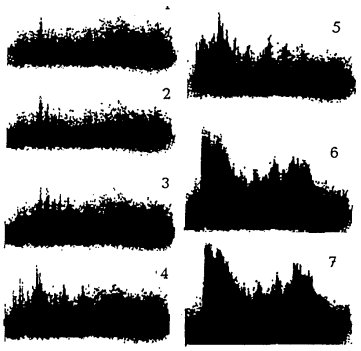

Fig. 9. Oscillations spectra vs. beam current I (mA)= 12 (1), 15 (2), 20 (3), 30 (4), 40 (5), 50 (6), 60 (7)

These pictures are shown that single mode generation near ω_p starts at I_1=12 mA, several frequencies start at I_2=15 mA, the continuous spectrum near ω_p appears at I_3=30 mA, a frequency near ω_H arises at I_4=40 mA and continuous spectrum near ω_H is formed at I_5=50 mA.

2. DISCUSSION

As is known, at the gas pressure of 10^{-6}-10^{-5} Torr, the neutralization of the electron beam by the ions (created by gas ionization) can occur. At increasing the gas pressure up to (1-2)*10^{-4} Torr, the secondary electrons are sufficiently accumulated and the BPD starts, see Figs. 1, 4, 5, 7. In 3rd experiment it was shown (Fig. 9) that the BPD starts at the plasma branch, as in [4-7] also.

We had measured the electron distribution function for longitudinal velocities and energies. From common notions, it is evident that dispersion of longitudinal velocities of secondary electrons can be large. By measurements, it was determined that, before starting BPD, the secondary electrons have the longitudinal mean energy ~10 eV, see Fig. 5a. This indicates possibility for kinetic type of beam-plasma instability at the BPD start. Really, the BPD starts such a way that the beam current magnitude is vice versa to the length of interaction distance: $I \propto L^{-1}$, see *Fig. 8*. There is an evidence that the instability has the kinetic increment $\gamma \propto n_b \propto I$. In fact, the BPD start depends on EM field amplitude increase along the system length to reach the critical value E_{cr} for the discharge: $E_{cr}=E_0 exp \gamma L$. So, if γL and IL *are const*, then $\gamma \propto I \propto n_b$.

The advanced BPD stage was theoretically studied in [8] where particle balance condition takes in account the secondary electrons accumulation (due to gas ionization by the electron beam), and their losses due to ambipolar diffusion (seen as main losses) and recombination. Unfortunately, at the BPD start conditions, for pressure of 10^{-4} Torr and low plasma density, the diffusion equation is invalid because the electron free path is sufficiently more then lengths of experimental systems, and the ion free path is sufficiently more then their transverse sizes.. In this case, for calculation of critical pressure p_{cr} we propose the balance equation for ions created by the electron beam and ones going away across the magnetic field through the lateral electron beam surface, whereas secondary electrons going away along the magnetic field:

$$\pi a^2 n_b v_b \sigma_i n_0 L = 2\pi a L n_i v_{\perp i}, \qquad (1)$$

where a – beam radius, n_b – electron beam density, v_b – beam velocity, σ_i – ionization cross-section, n_0 – neutral particle density, L – interaction length, n_i – ion concentration, $v_{\perp i}$ – ion transverse velocity. Supposing that $n_i=n_e$ (the quasi-neutrality condition), $n_e=n_b$ (the condition of maximum of the instability increment), and n_0=3.5*10^{16} p Torr, we receive relation for p_{cr} in the form:

$$p_{cr} = 2v_{\perp i} / 3.5*10^{16} a v_b \sigma_i \qquad (2)$$

The results of calculations are shown in the Table (here we use $W_{\perp i} \approx 1$ eV). The amount of calculated p_{cr} ($p_{cr} \sim 10^{-4}$ Torr) coincides with experimental data for the plasma branch but not coincides for the cyclotron one [2,3]. Latter may be explained as if ionization efficiency at the cyclotron branch is sufficiently increased.

References	Gas	W_b, keV	a, cm	σ_i, cm^2	$p_{cr.\,exp.}$ mTorr	$p_{cr..calc.}$ mTorr
[2]	H_2	0.58	0.13	3.9*10^{-17}	0.2	7.8
[3]	H_2	4.5	0.20	7.3*10^{-18}	2.0	9.2
[3]	N_2	4.5	0.20	2.5*10^{-17}	~0.1	0.59
[4]	Ar	0.50	0.15	1.8*10^{-16}	0.2	0.36
[5]	Air	1.2	0.65	8.1*10^{-17}	0.2	0.19
[6]	Ar	4.0	1.15	3.4*10^{-17}	0.1	0.09
1 exp	Air	10	0.50	1.4*10^{-17}	0.1	0.46
2 exp	Air	0.30	0.50	2.2*10^{-16}	0.2	0.12
3 exp	Air	2.0	1.50	5.3*10^{-17}	0.2	0.10

REFERENCES

1. Ya.B. Fainberg //*Atom. Energy (11).* 1961, p.313-322.
2. R.T. Targ, L.P. Levine // *J. Appl. Phys.* (*32).* 1961, p. 731 – 737.
3. E.A. Kornilov, O.F. Kovpik, Ya.B. Fainberg, I.F. Kharchenko // *Plasma Physics and Problems of Controlled Fusion*. 1965, № 4, Kiev, p. 145 – 151.
4. P. Hedwall // *J. Appl. Phys.* (*33).* 1962, p. 2426–2429.
5. E.G. Shustin, V.P. Popovich, I.F. Kharchenko // *JTP.* (*39).* 1969, № 6, с. 993 – 1000.
6. J. Jancharik, V. Kopecky, V. Piffl et al. // *Plasma Phys. & CTR./* Vienna, IAEA, 1969, V. 2, p. 733–748.
7. I.N. Onishchenko, A.K. Berezin, B.I. Ivanov, Ya.B. Fainberg // *Proc. of 17-th Intern. Symp. on Disch. & Electr. Insul. Vacuum.* Berkeley, 1996, p. 612-616.
8. P.M. Lebedev, I.N. Onishchenko, Yu.V. Tkach et al.// *Plasma Physics* (*2).* 1976, № 3, p. 407 – 413.

ЭКСПЕРИМЕНТАЛЬНОЕ ИССЛЕДОВАНИЕ НЕКОТОРЫХ СВОЙСТВ НАЧАЛЬНОЙ СТАДИИ ПУЧКОВО-ПЛАЗМЕННОГО РАЗРЯДА

В.И. Бутенко, Б.И. Иванов, В.П. Прищепов

При увеличении давления газа до (1-2)*10^{-4} Торр плотность плазмы резко возрастает благодаря пучково-плазменному разряду (ППР). При фиксированном давлении выше 2*10^{-4} Торр начало ППР зависит от длины взаимодействия L и тока пучка I: $I \propto L^{-1}$. Проведены измерения распределения электронов по скоростям СВЧ методом и многосеточным зондом. Условия старта ППР согласуются с теоретическими оценками.

ЕКСПЕРИМЕНТАЛЬНЕ ДОСЛІДЖЕННЯ ДЕЯКИХ ВЛАСТИВОСТЕЙ ПОЧАТКОВОЇ СТАДІЇ ПУЧКОВО-ПЛАЗМОВОГО РОЗРЯДУ

В.І. Бутенко, Б.І. Іванов, В.П. Прищепов

При збільшенні тиску газу до (1-2)*10^{-4} Торр щільність плазми різко підвищуется завдяки пучково-плазмовому розряду (ППР). При фіксованому тиску вище 2*10^{-4} Торр початок ППР залежить від довжини взаємодії L та струму пучка I: $I \propto L^{-1}$. Були проведені вимірювання розподілу електронів по швидкостям СВЧ методом та багатосітковим зондом. Умови старту ППР узгоджуються із теоретичними оцінками.